

April 1996

Magnetic and magneto-optical properties of $\text{Mn}_x\text{Pt}_{1-x-y}\text{Zn}_y$

Kurt W. Wierman

Seagate Corporation, Pittsburgh, PA

Roger D. Kirby

University of Nebraska-Lincoln, rkirby1@unl.edu

Follow this and additional works at: http://digitalcommons.unl.edu/physics_kirby



Part of the [Physics Commons](#)

Wierman, Kurt W. and Kirby, Roger D., "Magnetic and magneto-optical properties of $\text{Mn}_x\text{Pt}_{1-x-y}\text{Zn}_y$ " (1996). *Roger Kirby Publications*. 12.

http://digitalcommons.unl.edu/physics_kirby/12

This Article is brought to you for free and open access by the Research Papers in Physics and Astronomy at DigitalCommons@University of Nebraska - Lincoln. It has been accepted for inclusion in Roger Kirby Publications by an authorized administrator of DigitalCommons@University of Nebraska - Lincoln.

Magnetic and magneto-optical properties of $\text{Mn}_x\text{Pt}_{1-x-y}\text{Zn}_y$

Kurt W. Wierman and Roger D. Kirby

Behlen Laboratory of Physics and Center for Materials Research and Analysis, University of Nebraska, Lincoln, Nebraska 68588-0113

In this work we have prepared thin films of the ternary alloy $\text{Mn}_x\text{Pt}_{1-x-y}\text{Zn}_y$ by magnetron sputtering onto quartz substrates. We have found a wide range of compositions which are strongly ferromagnetic at room temperature. A transition from a cubic to tetragonal phase with decreasing Pt content is confirmed by x-ray diffraction. X-ray diffraction measurements also show a strong (001) reflection consistent with long range order along the c axis for the tetragonal phase. These films show large complex Kerr rotations (up to 0.7°) in the visible spectrum. This combined with their anisotropic structure suggests that they may be suitable for magneto-optic data storage applications.

© 1996 American Institute of Physics. [S0021-8979(96)16708-3]

INTRODUCTION

The ordered alloys of $\text{M}_x\text{Pt}_{1-x}$ ($\text{M}=\text{Cr}, \text{Mn}, \text{Fe}, \text{Ni}, \text{Co}$) have received considerable attention because of their interesting magnetic and magneto-optic properties.¹⁻⁵ For $x=0.25$ these alloys form the $L1_2$ (Cu_3Au) cubic structure where the magnetic atoms occupy the cube corners and the Pt atoms the face-centered sites. As x increases from 0.25 there is a continuous change in lattice parameters and by $x=0.5$ the alloys develop the $L1_0$ (CuAu) tetragonal structure with alternating layers of M and Pt atoms along the (001) direction. This appears to result from the geometrical requirements of ordered packing of Pt and M atoms of different sizes and not from electron concentration or Brillouin zone effects, as discussed by Brun *et al.* for $\text{M}=\text{Mn}$.² $\text{Mn}_x\text{Pt}_{1-x}$ alloys are known to undergo a transition from the cubic to a tetragonal structure for $x>0.38$; unfortunately, the increased number of antiferromagnetic Mn-Mn nearest-neighbor interactions induces a complex noncollinear magnetic structure.^{6,7} Kato *et al.*⁸ initially observed large Kerr rotation and ellipticity in thin films of MnPt_3 , but hysteresis loops showed an in-plane anisotropy concordant with its cubic structure. Our goal was to substitute a third nonmagnetic element into the Mn-Pt alloy to develop a ferromagnetic tetragonal structure. Thus, in this study ferromagnetic ternary alloys of $\text{Mn}_x\text{Pt}_{1-x-y}\text{Zn}_y$ were produced over a wide composition range ($x=0.17-0.29$, $y=0.00-0.13$), and their magnetic and magneto-optic properties were studied.

EXPERIMENT

Mn/(Pt-Zn) multilayers were prepared by dc magnetron sputtering onto room-temperature fused quartz substrates. The base pressure of the sputtering chamber was 4×10^{-7} Torr and the argon sputtering pressure was 2 mTorr. For the series of samples discussed here Pt and Zn were co-sputtered with a layer thickness held constant at 7 Å, while the Mn layer thickness was varied from 3 to 5 Å to obtain the desired $\text{Mn}_x\text{Pt}_{1-x-y}\text{Zn}_y$ composition ratios. The compositions of the as-deposited films were measured using x-ray fluorescence and found to be close to the nominal compositions. The total film thickness of each sample was 100 nm and each film was coated with a 100-nm-thick SiO_x protective overcoat. The as-deposited samples were subsequently annealed

in vacuum (6×10^{-6} Torr) at 850°C for 1 h to form the homogeneous crystalline $\text{Mn}_x\text{Pt}_{1-x-y}\text{Zn}_y$ alloy.

The saturation magnetization M_s and coercivity H_c of the $\text{Mn}_x\text{Pt}_{1-x-y}\text{Zn}_y$ films were measured at 300 K using an alternating gradient force magnetometer. The polar Kerr rotation and ellipticity spectra were measured in a 10 kOe applied field perpendicular to the film plane using a home-built system based on a photoelastic modulator. The Curie temperatures were obtained from Kerr rotation versus temperature measurements in an applied field of 7.1 kOe.

RESULTS AND DISCUSSION

Figure 1 shows the x-ray diffraction results for the annealed films of $\text{Mn}_{0.25}\text{Pt}_{0.75-y}\text{Zn}_y$ for several Zn concentrations. The splitting of the (110), (200), and (220) reflections shown in the $y=0.08$ sample indicates the formation of the tetragonal phase. The presence of the superlattice (001) peak is indicative of substantial long range order along the c axis. Figure 2 shows the a axis and c axis lattice parameters as a function of Pt concentration; for these data, x ranges from 0.17 to 0.29 and y ranges from 0.04 to 0.13. For concentrations greater than 69 at. % Pt the cubic phase with an average a -axis lattice parameter of 3.83 Å is present. This value is

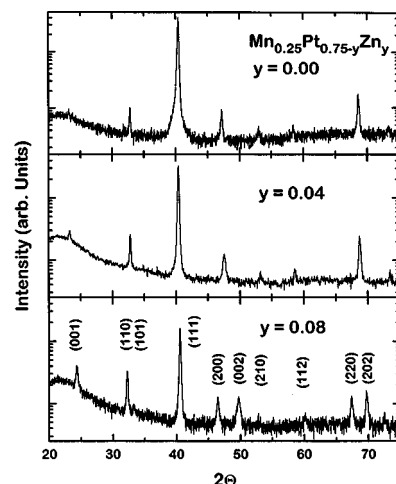


FIG. 1. X-ray diffraction results for $\text{Mn}_{0.25}\text{Pt}_{0.75-y}\text{Zn}_y$ with $y=0.00, 0.04$, and 0.08 .

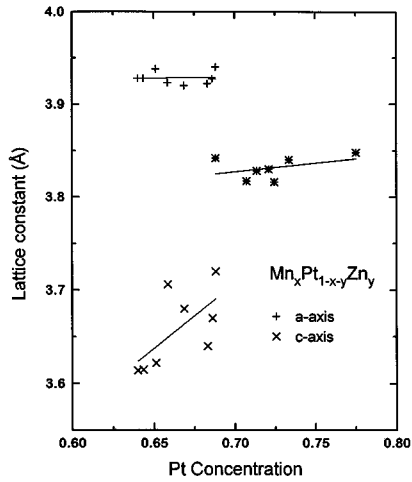


FIG. 2. Lattice parameters for varying Pt concentrations; x ranges from 0.17 to 0.29, y ranges from 0.04 to 0.13. The lines are drawn to aid the eye.

slightly smaller than the reported value of 3.89 Å for bulk MnPt_3 .⁹ Below 69 at. % Pt only the tetragonal phase is present with no indication of the cubic phase. The a -axis lattice parameter is 3.93 Å and is independent of Pt concentration, while the c -axis lattice parameter diminishes from 3.72 to 3.61 Å. At 69 at. % Pt the tetragonal and cubic structural phases co-exist indicating there is a narrow intermediate phase transition region as reported for bulk $\text{Mn}_x\text{Pt}_{1-x}$.⁷

As Mn-Mn nearest-neighbor interactions are antiferromagnetic the largest possible magnetic moment in the $L1_2$ structure is obtained at Mn concentration of 25%.^{7,10,11} For this reason the rest of this discussion will focus on samples with $x=0.25$. Figure 3(a) shows the room temperature in-plane hysteresis loops for $y=0.04, 0.06$, and 0.08 . A comparison of the perpendicular (not shown) and in-plane hys-

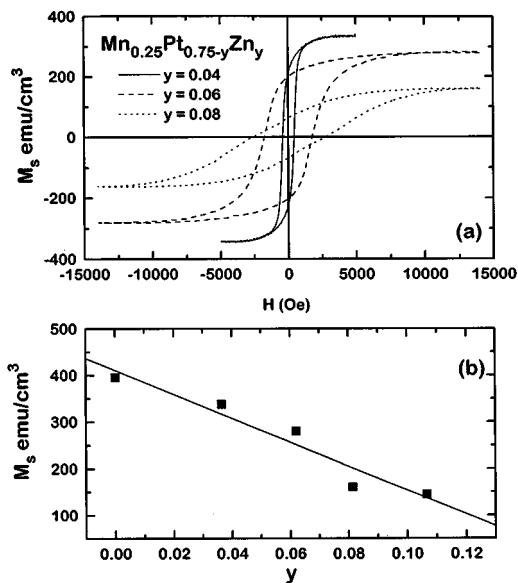


FIG. 3. (a) In-plane hysteresis loops for $\text{Mn}_{0.25}\text{Pt}_{0.75-y}\text{Zn}_y$. (b) M_s vs Zn concentration for $\text{Mn}_{0.25}\text{Pt}_{0.75-y}\text{Zn}_y$. The line is drawn to aid the eye.

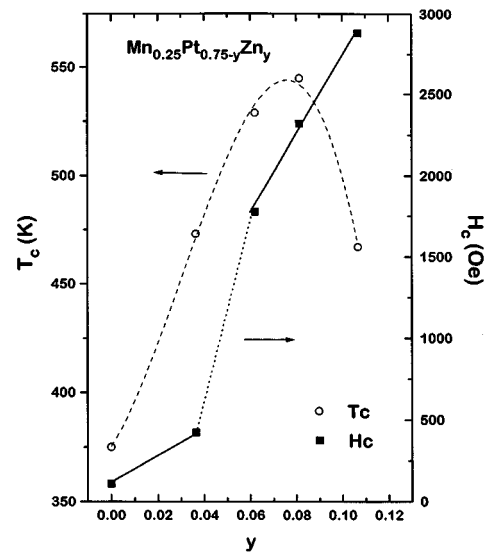


FIG. 4. T_c and H_c vs Zn concentration for $\text{Mn}_{0.25}\text{Pt}_{0.75-y}\text{Zn}_y$. The lines are drawn to aid the eye.

teresis loops indicates that the easy axis is not strictly in the plane of the film. Figure 3(b) shows that the saturation magnetization (M_s) decreases with increasing Zn content. Figure 4 shows the Curie temperature (T_c) and coercivity (H_c) as functions of Zn concentration. The initial slope of T_c vs Zn content is nearly the same as the slope found for T_c vs Mn content in $\text{Mn}_x\text{Pt}_{1-x}$.^{10,11} This suggests that the increase of T_c in the two systems has the same origin. It may be due to an increase in macroscopic exchange stiffness between Mn atoms due to a larger number of Mn-Mn nearest-neighbor interactions. Note there is a decrease in the c -axis lattice parameter for higher levels of Zn content which may contrib-

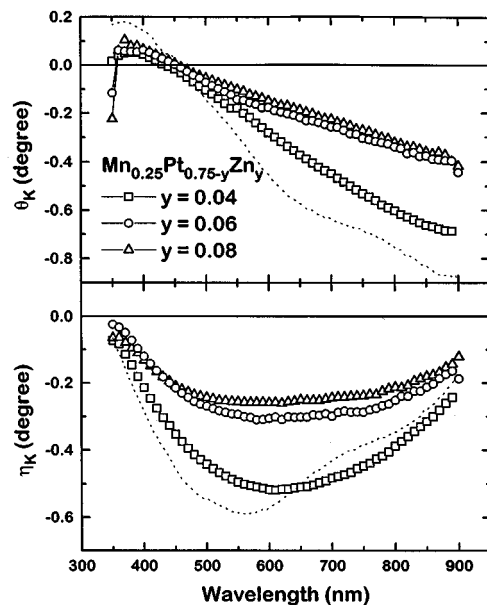


FIG. 5. Kerr rotation and ellipticity wavelength dependence for $\text{Mn}_{0.25}\text{Pt}_{0.75-y}\text{Zn}_y$ measured from the substrate side. Dotted line gives results for MnPt_3 measured from substrate side.

ute to the downward trend in T_c . The dramatic increase in coercivity appears to be associated with the structural change from cubic to tetragonal since all samples exhibiting the cubic phase have coercivities ranging from 75 to 660 Oe, while the samples with tetragonal phase have coercivities ranging from 1500 to 2900 Oe.

The room-temperature Kerr rotation (θ_K) and ellipticity (η_K) spectra (measured from the substrate side) for $\text{Mn}_{0.25}\text{Pt}_{0.75-y}\text{Zn}_y$, $y=0.04, 0.06, 0.08$, are shown in Fig. 5. The present spectra are similar to those of pure MnPt_3 (shown as dotted line) and the overall decreases in magnitude of θ_K and η_K correlate well with the decrease in M_s .

CONCLUSION

The magnetic and magneto-optical properties of $\text{Mn}_x\text{Pt}_{1-x-y}\text{Zn}_y$ alloy films have been investigated. We found that the formation of the tetragonal phase primarily depends on the Pt content, but the addition of Zn influences the formation of a ferromagnetic tetragonal phase with a fairly large saturation magnetization. The crystallographic sites of the Zn atoms have not been determined, but diffraction suggests a preferential layering of the Pt atoms to form alternating (Mn-Zn-Pt)/Pt layers along the (001) direction. No (100) diffraction peak was observed in the tetragonal phases. This together with the rapid decrease in M_s with Zn

content seem to indicate a large degree of disorder in the (Mn-Zn-Pt) layer. Such disorder would lead to an increase in the number of Mn-Mn antiferromagnetic exchange interactions.

ACKNOWLEDGMENTS

We gratefully acknowledge the support of the National Science Foundation under grants OSR-9255225 and DMR-9222976, and support from the Center for Materials Research and Analysis of the University of Nebraska.

- ¹A. J. P. Meyer and M. J. Besnus, Phys. Status Solidi B **58**, 533 (1973).
- ²K. Brun, A. Kjekshus, and W. B. Pearson, Philos. Mag. **10**, 291 (1964).
- ³J. Crangle and J. A. Shaw, Philos. Mag. **7**, 207 (1962).
- ⁴M. C. Cadeville, C. E. Dahmani, and F. Kern, J. Magn. Magn. Mater. **54-57**, 1055 (1986).
- ⁵D. Treves, J. T. Jacobs, and E. Sawatzky, J. Appl. Phys. **46**, 2760 (1975).
- ⁶A. F. Andresen, A. Kjekshus, R. Møllerud, and W. B. Pearson, Philos. Mag. **11**, 1245 (1965).
- ⁷S. K. Sidorv and S. F. Dubinin, Phys. Met. Metallogr. USSR **24**, 90 (1967).
- ⁸T. Kato, H. Kikusawa, S. W. Iwata, S. Tsunashima, and S. Uchiyama, J. Magn. Magn. Mater. **140-141**, 713 (1995).
- ⁹B. Antonini, F. Lucari, F. Menzinger, and A. Paletti, Phys. Rev. **187**, 611 (1969).
- ¹⁰M. Auwärter and A. Kussman, Ann. Phys. **7**, 169 (1950).
- ¹¹K. W. Wierman and R. Kirby, these proceedings.